Global cloud-permitting simulations of Typhoon Fengshen (2008)

Tomoe Nasuno[1]*, Hiroyuki Yamada[2], Masuo Nakano[1], Hisayuki Kubota[3], Masahiro Sawada[4], and Ryuji Yoshida[5]

*[1] Japan Agency for Marine-Earth Science and Technology, [2]Faculty of Science, University of the Ryukyus,[3]Atmosphere and Ocean Research Institute, The University of Tokyo, [4]Meteorological Research Institute,[5]RIKEN, Advanced Institute for Computational Science, *Tomoe Nasuno: nasuno@jamstec.go.jp*

Acknowledgements

This work was supported by JSPS KAKENHI Grant Numbers JP26400475. All the simulations are conducted on the Earth Simulator at JAMSTEC.

Motivation

The tropical cyclone (TC) genesis over the western North Pacific (WNP) occurs under multiple effects of different temporal and spatial scales; Asian summer monsoon (e.g., low-level circulation, convective activity), boreal summer intraseasonal oscillation (BSISO), synoptic scale disturbances (e.g., Rossby wave trains, TD-type waves, easterly waves), upper tropospheric troughs, and mesoscale convective systems (MCS). The objective of the present study is to gain our understanding of the effects of the multiple factors on the TC genesis. A case of Typhoon Fengshen (2008) is investigated by a set of 3.5-km mesh global non-hydrostatic simulations, where the multi-scale processes are seamlessly represented in a unified framework.

Model and experimental design (Nasuno et al. 2016)

Nonhydrostatic ICosahedral Atmospheric Model (NICAM) (Satoh et al. 2014)

- horizontal mesh size: 3.5 km
- vertical levels: 40L (0 m ~ 38,000 m)
- cloud mycrophysics : NSW6 (Tomita 2008)
- turbulence : MYNN level 2 (Nakanishi and Niino 2004) (Noda et al. 2010)
- radiation : MSTRN X (Sekiguchi and Nakajima 2008)
- ocean : slab model (SST nudged to NOAA OI SST)
- land surface : bucket model/MATSIRO
- initial data: ECMWF YOTC analysis (0.5x0.5)
- integration: 15-21/06/2008 (TS genesis: 19/06/2008)

Table 1. List of simulation cases

case	Initial data	Cloud microphysics
E_mp1	ECMWF YOTC	mp1: cloud ice sedimentation (Hashino et al. 2013)
E_mp2	ECMWF YOTC	mp2: default (Nasuno 2013)
E_mp3	ECMWF YOTC	mp3: tuned upper-tropospheric clouds for cloud-radiative balance (Kodama et al. 2015)
E_mp4	ECMWF YOTC	mp4: reduced terminal velocity of precipitating condensates for MJO simulation (Miura et al. 2015)
N_mp2	NCEP FNL	mp2: default (Nasuno 2013)

* Tuning for mp3 and mp4 were for the 14-km mesh simulations

References

Geng, B., K. Yoneyama, R. Shirooka and M. Yoshizaki, 2011, J. Meteor. Soc. Japan, 89A, 1-25.
Hashino, T., M. Satoh, Y. Hagihara, T. Kubota, T. Matsui, T. Nasuno, and H. Okamoto,2013, J. Geophys. Res. Atmos., 118, doi:10.1002/jgrd.50564.
Katsumata, M., H. Yamada, H. Kubota, Q. Moteki, and R. Shirooka, 2013, Mon. Wea. Rev., 141, 690-706.
Kodama, C. and co-authors, 2015, , J. Meteor. Soc. Japan, 93, 393-424.
Miura, H., T. Suematsu, and T. Nasuno, 2015, J. Meteor. Soc. Japan, 93A, 115-137.
Nakanishi M, and H. Niino, 2006, Boundary-Layer Meteorol 119, 397–407.
Nasuno, T., 2013, SOLA, 9, 69-73.
Nasuno, T., H. Yamada, M. Nakano, H. Kubota, R. Yoshida, 2016, Geoscience Letters, 3:32, DOI 10.1186/s40562-016-0064-1.
Noda A, K. Oouchi , M. Satoh, H. Tomita, S. Iga, and Y. Tsushima, 2010, Atmos Res 96, 208–217.
Satoh, M. and co-authors, 2014, Progress in Earth and Planetary Science, 1, 18. doi:10.1186/s40645-014-0018-1.
Sekiguchi, M. and T. Nakajima, 2008, J.Quantitative Spectroscopy and Radiative Transfer 109, 2779–2793.
Tomita 2008, J Meteor Soc Japan 86A, 121–142.

TC case: Fengshen (2008)

Fengshen (2008) were generated during the onset period of the WNP monsoon (Geng et al. 2011) and an active phase of BSISO (Katsumata et al. 2013). The 850-hPa flow fields on 15 June indicate a large-scale cyclonic gyre associated with the BSISO (Fig. 1a, 1b), and moisture was accumulated within the gyre (Fig. 1c, 1d). Interestingly, differences between ECMWF YOTC and NCEP FNL are found in moisture and flow fields that might affect convective behavior.

In this large-scale environment, Fengshen was detected as TD at 06 UTC 17 June. The SLP started decreasing on 18 June, and reached the minimum value (945 hPa) on 21 June (Fig. 2, JTWC best track).

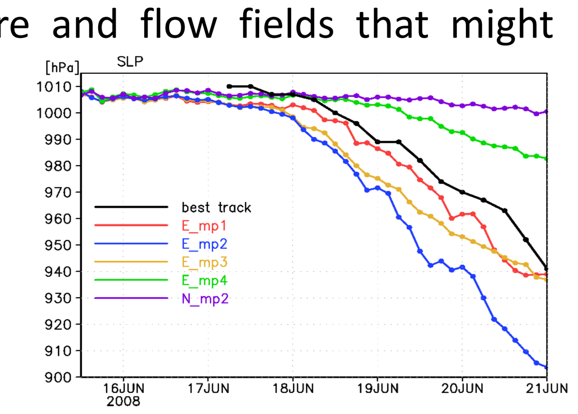

Fig. 2. Time series of central sea level pressure (SLP) in the best track (black) and simulations (color).

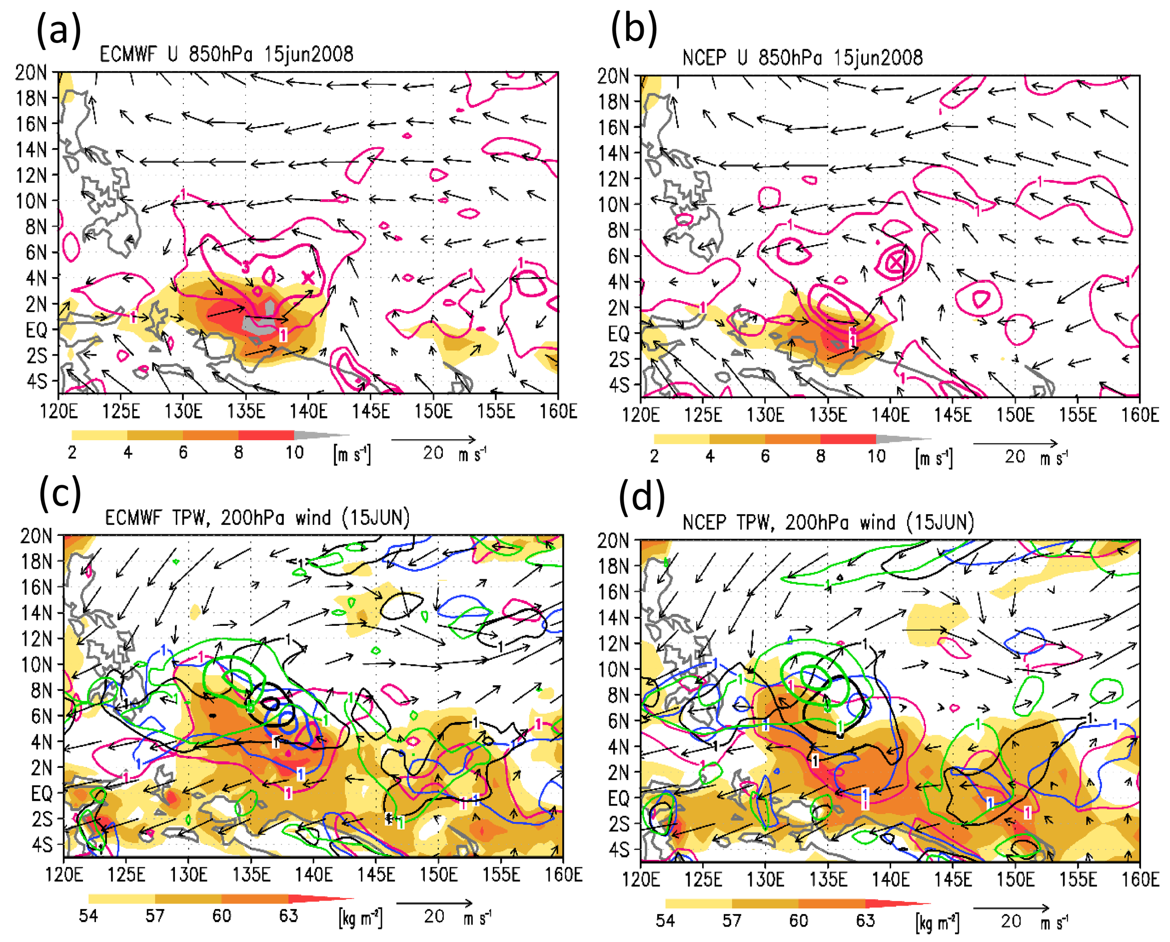

Fig. 1. (a) (b) The 850-hPa zonal velocity (shading), relative vorticity (red contour; 1, 3 and 5× 10^{-5} s^{-1}), and wind vectors, (c) (d) column integrated water vapor (shading) and 200-hPa wind vectors, at 0000 UTC on 15 June 2008 in the ECMWF YOTC (a) (c) and the NCEP FNL (b) (d). Contour lines of 850-hPa relative vorticity averaged between 6-hours before and after 0000 UTC on 15 (red), 16 (blue), 17 (black), and 18 (green) June 2008 are also depicted in (c) (d) (1, 5, and 10 × 10^{-5} s^{-1}). Crosses in (a) (b) indicate the location of the center of the incipient disturbance at 900 hPa.

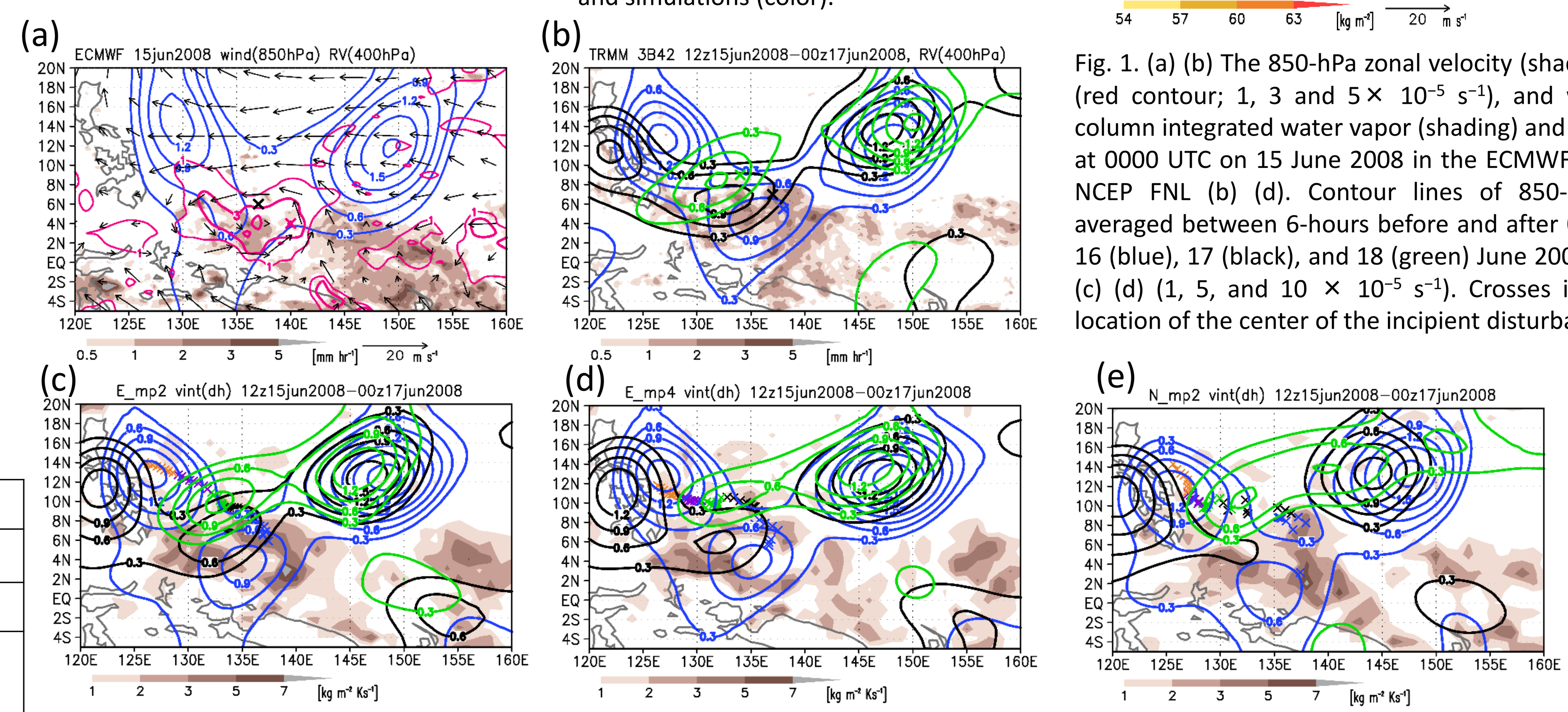

Fig. 3. (a) The smoothed 400-hPa relative vorticity (blue), 850-hPa wind vectors and relative vorticity (red) at 0000 UTC 15 June 2008 in the ECMWF YOTC with the precipitation rate (1200 UTC 13 June - 0000 UTC 15 June) in TRMM 3B42v7 (shading). (b) Smoothed 400-hPa relative vorticity at 0000 UTC 16 (blue), 17 (black), and 18 (green) June 2008 in the ECMWF YOTC with the precipitation rate (1200 UTC 15 June - 0000 UTC 17 June) in TRMM 3B42v7 (shading). Same as (b), but for (c) E_mp2, (f) E_mp4, and (e) N_mp2 (z = 7.6-km), with the vertically integrated latent heating rate (shading). The unit of relative vorticity is 10^{-5} s^{-1} and only positive values are shown. Crosses indicate the center of the incipient disturbance on 15 (red), 16 (blue), 17 (black), 18(green), 19 (purple), and 20 (orange) June 2008.

Large-scale processes

On 15 June 2008 (initial date of simulation), positive vorticity anomalies (troughs) developed in the subtropical middle to upper troposphere and overlapped the lower tropospheric gyre (Fig. 3a). In the subsequent three days, the middle tropospheric trough intensified and migrated northwestward (Fig. 3b). The center of the low-level incipient vortex was located on the northeastern rim of the vorticity maximum. Prior to the intensification of the middle tropospheric vorticity, convective activity was enhanced in the broad domain corresponding to the lower tropospheric large-scale gyre.

In E_mp2, these were successfully simulated (Fig. 3c). In E_mp4, a weak trough was formed after 16 June, with smaller latent heat release than in E_mp2 (Fig. 3d). In N_mp2, the middle tropospheric trough was weak, and less coherent to the latent heat release and lower tropospheric gyre (Fig. 3e). These results indicate that the large-scale latent release associated with the lower tropospheric conditions (e.g., the active period of BSISO) was important to the growth of the middle tropospheric trough and subsequent development of TC.

Summary

global 3.5-km mesh simulations of the genesis of Fengshen (2008)

1. In three runs initialized with the ECMWF YOTC, **a middle tropospheric trough developed by a large-scale latent heat release**, which enabled **the successive occurrence of deep convective events within the 50-km radius**, leading to a **TC formation**.
2. In the run with **weaker latent heating in the lower troposphere**, the **trough was weak** and **TC formation** was significantly **delayed**.
3. In the run initialized with NCEP FNL, **collocation between latent heat release and the large-scale gyre was less evident**, and **neither the trough nor a TC developed**.

These results suggest that **the superposition of large-scale disturbances in the lower and middle troposphere** and their **linkage through convective enhancement** played an important role in the genesis of Fengshen by preconditioning **the establishment of a deep upright inner core**.

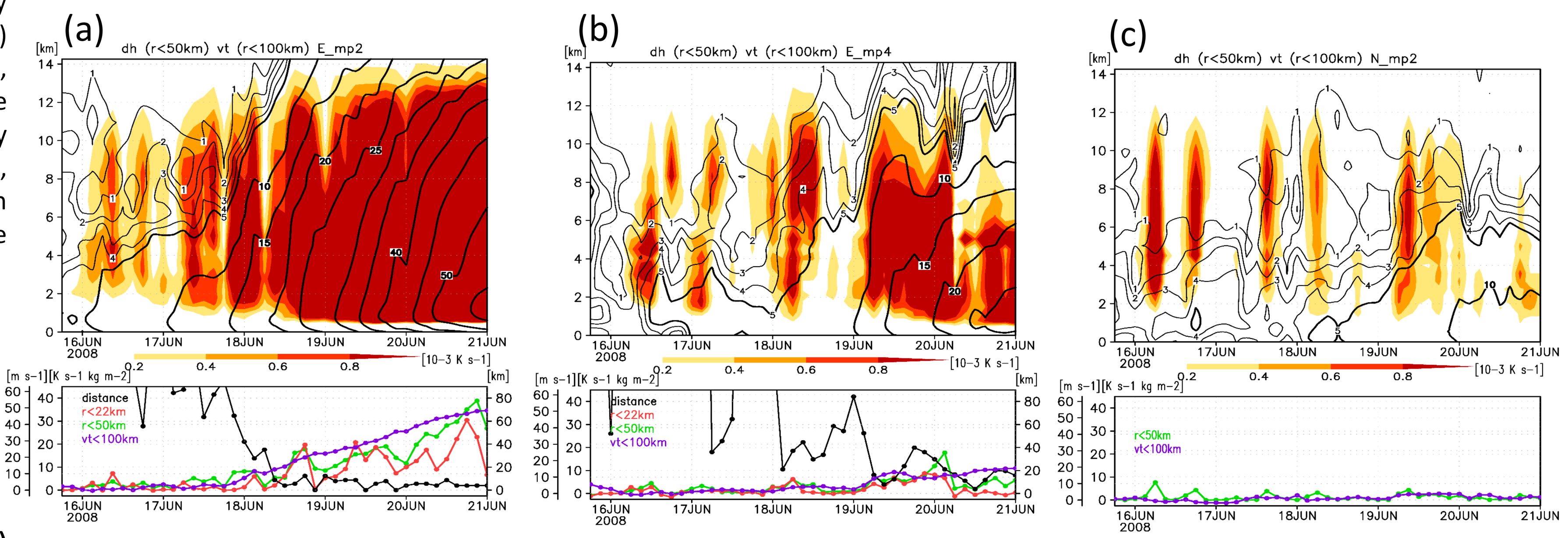

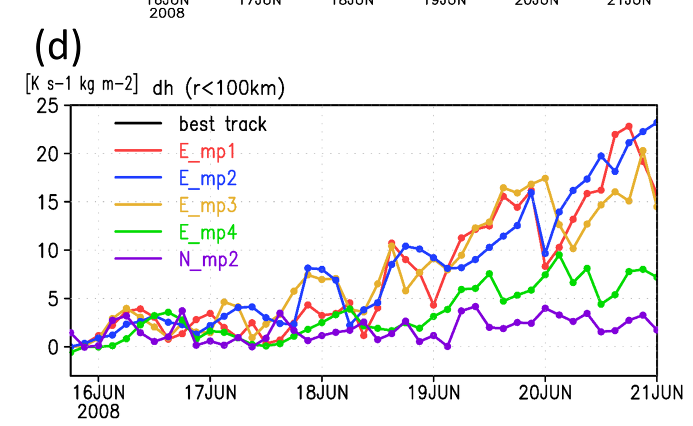

Fig. 4. (upper) Height–time sections of the latent heating rate (shading; 10^{-3} K s^{-1}) and tangential velocity (contour; m s^{-1}) averaged within the 50-km and 100-km radius, respectively, (lower) time series of the vertically integrated latent heating rate averaged within the 22-km (red) and 50-km (green) radius, the 7.6-km tangential wind averaged within the 100-km radius (purple), and distance between the center of the vortex at the 1.0- and 7.6-km altitude (black) in (a) E_mp2, (b) E_mp4, and (c) N_mp2. (d) Time series of the vertically integrated latent heating rate within the 100-km radius.

Formation of the TC inner core

Figure 4 presents the time evolution of the inner core of the simulated storm. Deep latent heating associated with convective events within the 50-km radius occurred at 12 hours or at shorter intervals during 16–17 June in E_mp2 (Fig. 4a). An increase in the azimuthal mean tangential wind in the middle troposphere occurred simultaneously or several hours after the deep convective events. An increase in the tangential wind was less clear in E_mp4 and N_mp2 in this period (Fig. 4b, 4c). This is attributable to the weakness of the large-scale vorticity (Fig. 3) that preconditioned the intensification of the TC inner core. In E_mp2, an abrupt increase in the column integrated latent heat release occurred over a 1~1.5-day period around 18 June (Fig. 4a, 4d). Concurrent with the outbreak of the latent heat release, the distance between the lower and middle tropospheric vorticity maximum sharply decreased, and the middle tropospheric tangential wind was abruptly accelerated. This indicates the establishment of an upright deep TC inner core within the large-scale vorticity fields.